

## Interactions of High Energy Nucleons with Nuclei.\* Part I

G. BERNARDINI, E. T. BOOTH, AND S. J. LINDENBAUM†  
*Columbia University, New York, New York*

(Received October 23, 1951)

Goldberger attempted to explain the interaction of high energy nucleons ( $\sim 90$  Mev) with heavy nuclei on the basis of a nucleonic cascade in a nucleon Fermi gas. The experimental test of this model was indecisive. In order to check the model at the higher energies available at the Nevis cyclotron, the interactions of 300–400 Mev protons and neutrons with the G-5 emulsion nuclei were analyzed. The experimental results are given and general evidence for the nucleonic cascade mechanism is presented.

### I. INTRODUCTION

THE ideas set forth by Serber<sup>1</sup> concerning the inelastic interaction of a high energy nucleon with a heavy nucleus were extended by Goldberger<sup>2</sup> and developed into a detailed model for the behavior of a nucleon inside nuclear matter. The heavy nucleus was represented by a zero temperature Fermi gas of nucleons in a potential well of depth equal to the maximum Fermi energy plus the average nucleon binding energy. The incoming high energy nucleon was considered to be well localized (since its wavelength is much less than nuclear diameter) and to interact with the nucleon gas by a series of single nucleon-nucleon scatterings. The free nucleon-nucleon scattering cross sections were employed but were appropriately reduced by the Pauli exclusion principle, which excludes scatterings into momentum states within the filled Fermi sphere. The struck nucleons interacted similarly and in this way an internal nucleonic cascade was generated which proceeded until either the moving nucleons reached the edge of the nucleus and escaped or fell below the nuclear barrier (including Coulomb) and were thermally captured. Finally, there were some immediately ejected fast nucleons and a thermally excited nucleus which subsequently evaporated in a manner described by the Weisskopf<sup>3</sup> thermodynamical theory.

To treat complex cascades of this type and retain all the natural statistical fluctuations, Goldberger employed the Monte Carlo method. The evaluations were performed for the interaction of 90-Mev neutrons with a Pb nucleus. An experimental check of Goldberger's evaluation by Hadley and York<sup>4</sup> was interpreted to be at best only in partial qualitative agreement. The discrepancies may have been caused by the failure of the model at these low energies for which pick-up effects, multiple nucleon interactions, and refraction effects could be important. However, the assumed  $p$ - $p$  and  $n$ - $n$  cross sections which were later shown to be erroneous and some approximations in the calculations

are also at least partly responsible. The broadness of the neutron beam energy spectrum and the difficulties in comparing in detail the calculations and the experiment could also be partly responsible for the differences.

The Fermi gas nuclear model has had a fair degree of success in explaining nuclear shell structure, and has also been successful in explaining nuclear transparency via the concept of a mean free path in nuclear matter.<sup>5</sup>

The Goldberger model is essentially based on extension of these concepts. Therefore, in spite of its apparent failure, or perhaps it is better to say indecisive test at 90 Mev, it was felt that it is worthwhile to check the model at the higher energies of 300–400 Mev protons and neutrons available at the Nevis cyclotron.

The model would be expected to be intrinsically better at these energies since the free nucleon scattering cross sections become much less than the nucleon cross section, even without the action of the Pauli exclusion principle, and also edge refraction effects, etc., become much less important.

Also, with a bombarding energy in the region of 300–400 Mev it is still possible to neglect meson production,<sup>6</sup> but at the same time one would expect rather large internal nucleonic cascades which provide a more definitive check of the basic features of the model.

The recent determinations of  $n$ - $p$  and  $p$ - $p$  scattering cross sections up to energies of about 300–350 Mev make a new set of Goldberger type of evaluations possible.

Since the calculations yield the detailed information about the properties of the nucleons emanating from the individual nuclear events, a most sensitive comparison of the theory and experiment can be made when the individual nuclear events are studied experimentally, and their fluctuations as well as the over-all mean distributions are compared to the theory. This is possible with the electron sensitive emulsions since all charged particles emanating from the individual nuclear events are visible.

\* This project was jointly supported by the ONR and AEC.

† Now at the Brookhaven National Laboratory, Upton, New York.

<sup>1</sup> R. Serber, Phys. Rev. **72**, 1114 (1947).

<sup>2</sup> M. L. Goldberger, Phys. Rev. **74**, 1269 (1948).

<sup>3</sup> V. Weisskopf, Phys. Rev. **52**, 295 (1937).

<sup>4</sup> J. Hadley and H. York, Phys. Rev. **80**, 345 (1950).

<sup>5</sup> Fernbach, Serber, and Taylor, Phys. Rev. **75**, 1352 (1949).

<sup>6</sup> An experimental estimate of meson production cross sections by the 385-Mev Nevis proton beam has been made by Block, Havens, and Passman [Phys. Rev. **83**, 167 (1951)]. These results indicate that less than 2–3 percent of the 350–400 Mev proton-induced nuclear interactions should be affected by meson production.

There is the disadvantage of a mixture of heavy (Ag-Br) and light (gelatin) nuclei. However, this has not proven too serious since it has been calculated (and checked experimentally) that at least 80 percent of the inelastic nuclear events occur in Ag-Br nuclei of average mass number  $\sim 100$ . There are other ways of separating the gelatin effects which will be discussed later.

## II. PROTON-INDUCED NUCLEAR INTERACTIONS

### A. Experimental Procedure

Four-hundred-micron Ilford G5 plates (3 inches by 1 inch) were exposed to the proton beam of the Nevis cyclotron. The exposures were made inside the vacuum chamber with the emulsion surface parallel to but  $1\frac{1}{4}$  inches below the median plane. The plates were positioned such that the 3-inch dimension was bisected by the  $n=0.2$  point, and with only the arc filament operating, the R.F. was switched on for a 5-sec period.

The plates were developed using the amidol, two-temperature method.<sup>7</sup> The development was uniform and a minimum ionization grain density of 33 grains per 100 microns was observed. The halves of the plates inside the  $n=0.2$  point were covered by a more or less uniform flux of  $2-4 \times 10^6$  fast proton tracks per  $\text{cm}^2$  with an average length in the emulsion of about 5 mm. These tracks were almost parallel to the beam direction with an angular distribution of half-width equal to one degree.

Since the grain density of 400-Mev protons changes very slowly with energy, it was not practicable to determine the energy spectrum of the protons by grain counting. However, a check of the mean energy by grain density measurements gave the expected value of 1.5 minimum corresponding to 400 Mev.

A finer method of obtaining the energy spectrum was developed using cyclotron beam orbit theory. A statistical correlation between the angular distribution of the proton tracks in the plates and the maximum energy spread in the beam was developed. An evaluation based on this fixed the energy spectrum between the limits of 350–400 Mev. Actually, it may well be narrower than this, since part of the angular spread in the plate is because of Coulomb scattering in the plate, and this was not corrected.

Another approach to justify this estimate was an analysis of how the beam is lost as a function of radial and vertical oscillations introduced by the multiple traversals in our target geometry. The results of this calculation supported the previous estimate of a proton beam spectrum between 350–400 Mev. An independent analysis of multiple traversal phenomena was performed by Knox<sup>8</sup> and was checked experimentally at Berkeley by a different method. The results obtained were in agreement with the above conclusions.

<sup>7</sup> Dilworth, Occhialini, and Vermaesen, Bulletin du Centre de Physique Nucleaire, Bruxelles 13a, part I (1950).

<sup>8</sup> W. Knox, Phys. Rev. 81, 693 (1951).

### B. Terminology

To observe all inelastic nuclear interactions and to determine the corresponding mean free path in emulsion, proton tracks were individually followed. Only those regions of tracks at least 50 microns from either surface were used. In 1820 cm of proton track 34 inelastic events were observed. All observable nuclear events were recorded and classified phenomenologically in the following categories:

#### *Star Production*

The sudden ending of the incoming proton at a point from which either 2 or more tracks of any given grain density emerge, or only one track of grain density  $> 3$  times minimum emerges was defined as star production. Twenty-nine cases of star production were observed. The star tracks, to adhere to the usual notation, were classified into three groups.

(1) Gray—denotes prongs of grain density less than three times minimum.

(2) Sparse black—denotes prongs of grain density between about three and six times minimum.

(3) Black—denotes prongs of grain density greater than about six times minimum. In order to exclude recoil nuclei only those black prongs of range greater than 10 microns were recorded.

These grain density ranges correspond, respectively, to proton energies greater than 100 Mev, between 100 Mev and 30 Mev, and less than 30 Mev.

#### *Scatterings*

A scattering was defined as a sudden change of direction of the incoming proton with the scattered proton remaining as a gray prong (grain density  $< 3$  times minimum). Seven scatterings by a polar angle of less than  $10^\circ$  with no apparent change in grain density were observed. These are attributable to elastic shadow and Coulomb scatterings. Three scatterings greater than  $10^\circ$  were observed and these are probably attributable to inelastic nuclear interactions, since the cutoff of the elastic shadow scattering for the emulsion elements has been calculated to be about  $10^\circ$ . The cross section for Coulomb scatterings greater than  $10^\circ$  is negligible compared to the geometric.

#### *Stops*

Sudden disappearance of a proton in a region of the emulsion of full sensitivity was defined as a stop. Two cases were observed and both had a characteristic blob which is probably a nuclear recoil.

The above results are summarized in Table I.

### C. Mean Free Path for Inelastic Nuclear Interactions

The experimental measurement error in proton track length is estimated to be of the order of 1 percent.

TABLE I. Distribution of events found scanning along proton tracks.

Event	Scat- tering >10°	Stops in flight	Stars <sup>a</sup>							Prongs	
			0	1	2	3	4	5	6	7	
Number	3	2	1	8	5	4	5	4	0	2	

<sup>a</sup> Stars are classified according to the number of non-gray prongs, i.e., number of black plus sparse black prongs.

The mean free path for all inelastic nuclear interactions is

$$\lambda_{in} = 1820/34 = 54 \pm 9 \text{ cm.}$$

This result clearly indicates the phenomenon of nuclear transparency for 350–400 Mev protons, since the mean free path for G5 emulsion corresponding to a geometrical nuclear cross section is 25 cm. In the case of neutrons the phenomenon has been clearly established by Cook *et al.*<sup>9</sup> for 90-Mev neutrons and later by Fox *et al.*<sup>10</sup> and DeJuren<sup>11</sup> for 270-Mev neutrons.

To obtain large enough statistics for the distribution of the events by scanning along individual proton tracks would have been prohibitive from the point of view of time, and so a standard scanning “per area” with high resolution oil objective was employed. This scanning also gave us a check of the cross section based on better statistics. It was found by cross-checking two observers that all stars of at least one or more non-gray prongs would be reliably and consistently found in the normal scanning method. Therefore, a determination of the cross section for one or more non-gray prong stars was made using the method of track length sampling in conjunction with the normal scanning.

Based on 404 stars, a mean free path of  $\lambda_{star} = 56 \pm 9$  cm was found, where the errors include the statistical one ( $\pm 3$ ) and the experimental one ( $\pm 6$ ). In order to obtain the mean free path for all inelastic nuclear interactions, corrections must be made in some way for the events missed in the normal scanning. It was observed that the experimental numbers of 1, 2, and 3 prong stars (of the 404) are about the same. It therefore seems reasonable to assume the same frequency for the events missed (which correspond to the zero prong stars).<sup>12</sup> This leads to a multiplying factor of  $0.81 \pm 0.06$  which is consistent with the data of Table I, showing that 28 of the 34 inelastic events listed are of the type which would be seen in normal scanning. Using this factor one finds as the mean free path for all inelastic nuclear interactions  $\lambda = 45 \pm 9$  cm. This agrees with the value found by scanning along individual tracks. The corresponding cross section is  $\sigma = (0.56 \pm 0.11) \sigma_{geom}$ .

<sup>9</sup> Cook, McMillan, Peterson, and Sewell, Phys. Rev. **75**, 7 (1949).

<sup>10</sup> Fox, Leith, Wouters, and MacKenzie, Phys. Rev. **80**, 23 (1950).

<sup>11</sup> J. DeJuren, Phys. Rev. **80**, 27 (1950).

<sup>12</sup> The term, “zero prong star” would refer to what was previously defined as a stop or a scattering and also to stars consisting of two or more gray prongs only.

Inelastic cross section measurements<sup>9,10</sup> with high energy neutrons have shown that the total inelastic cross section for light and heavy nuclei can be approximately computed<sup>5</sup> by considering the nucleus as a Fermi gas of noninteracting nucleons and attributing to it an absorption coefficient based upon the density of nucleons and the experimental scattering cross sections, which are appropriately reduced to satisfy the Pauli exclusion principle.

A calculation of this type for the interaction of 350–400 Mev protons with emulsion was performed by extrapolating experimentally measured cross sections to 350–400 Mev. The calculated inelastic cross section for emulsion is  $\sigma_{in} \approx 0.6 \sigma_{geom}$ .<sup>13</sup> This agrees very well with the measured value.

Using the results of this calculation, the ratio of the total inelastic cross section of the Ag-Br to that of the gelatin in the emulsion is 4:1. Therefore, it is to be expected that about 80 percent of the stars are Ag-Br events.

#### D. Proton Star Characteristics and Distribution Curves

Only those stars which clearly exhibited an incoming proton of the proper grain density and directed in the well-collimated region of  $\pm 2^\circ$  from the beam direction

TABLE II. Proton star characteristics.

A. Mean prong numbers				
Type of prong	Black	Gray	Sparse black	
Mean prong number	3.1 ± 0.15 correcting for zero prong stars: 2.5 ± 0.2	0.42 ± 0.04	0.35 ± 0.04	
B. Gray prong distribution.				
Number of gray prongs	0	1	2	3 4
Percentage of events	(57 ± 4)%	(40 ± 4)%	(2.5 ± 1)%	0 0
C. Fast (sparse black or gray) prong distribution.				
Number of fast prongs	0	1	2	3 4
Percentage of events	(35 ± 3)%	(54 ± 4)%	(9 ± 2)%	(1.7 ± 0.7)% 0

<sup>13</sup> This result is not very sensitive to the extrapolation for the following reasons. The  $p$ - $p$  cross section is known and does not change from 120 Mev to 340 Mev [Chamberlain, Segrè, and Weigand, Phys. Rev. **81**, 661 (1950)], and therefore should very probably be the same at 400 Mev. The  $n$ - $p$  cross section is known from 40 to 270 Mev [Hadley, Kelly, Leith, Segrè, Weigand, and York, Phys. Rev. **75**, 351 (1950); Kelly, Leith, Segrè, and Weigand, Phys. Rev. **79**, 96 (1950)], and is continuously decreasing with energy somewhat more slowly than a  $1/E$  law. Provided that it does not change its behavior too drastically in the region of 270–400 Mev, the calculated result will be close to the measured one, because the nuclear transparency is a slowly varying function of cross section in this region.

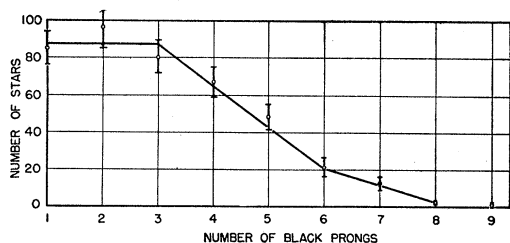


FIG. 1. Black prong distribution curve based on 412 stars induced in G-5 emulsion by 350-400 Mev protons.

were considered. The identification of different types of prongs was made visually after the training of the observers. A systematic check of the gray-sparse black border by grain counting showed that the distinction was included in the range 80-120 Mev.<sup>14</sup> The sparse black to black border was checked by using the range-grain density relations found for prongs ending in the emulsion and  $\pi$ - $\mu$  decays. The maximum variation in the black to sparse black classification was from 25-35 Mev. The lower end of this range was always identifiable as black and the upper end as sparse black.

Hereafter for simplicity the border divisions will be considered to be at 30 Mev and 100 Mev. Gray or sparse black prongs will be called "fast prongs."

In Fig. 1 the proton star distribution curve is given as a function of the number of black prongs only. It is based on 412 stars.

Figure 2 presents the percentages of stars in each star size group (determined by the number of black prongs) which exhibit outgoing fast prongs. The solid curve represents stars with at least one outgoing gray prong. The dotted curve represents stars with at least one outgoing gray or sparse black prong. Table II presents characteristic data.

These distribution curves and data can be considered as primarily representative of the processes occurring in Ag-Br nuclei. As previously calculated, the percentage of events occurring in gelatin is at most 20 percent. An experimental determination of the ratio of the gelatin events to Ag-Br events for 300-Mev neutrons incident upon G5 emulsion has been performed by Blau,<sup>15</sup> employing stratified emulsions. The result was that only  $17 \pm 3$  percent of the visible stars induced in the emulsion occur in gelatin. The gelatin star distribution curve was found to be predominantly confined to the small stars (<5 black prongs). Only about 5 percent of the large stars (5 or more black prongs) were found to be attributable to gelatin events. Hence, the large stars are almost exclusively Ag-Br events.

A similar result might reasonably be expected for proton-induced stars. This will become evident when neutron and proton stars are compared later and are shown to be equivalent.

<sup>14</sup> The tracks were followed completely. In the doubtful cases the grains were counted.

<sup>15</sup> M. Blau (private communication). We are very much indebted to Dr. Blau for this information.

The effective cutoff of the black prong distribution curve is at about 8 black prongs. Assume that this represents the complete transfer of 400 Mev to an Ag-Br nucleus and that the relationship is linear. Then an approximate estimate of the average energy transferred to the nucleus per black prong is 50 Mev. This is not to be construed as pure thermal energy transfer, but merely as an energy dissipation in low energy nucleons or groups of nucleons.

The cutoff of stars with a *gray* prong at 6 prongs also supports this view, since a 6-prong star would represent 300-Mev energy transfer, which would leave 100 Mev, or just about enough energy for a border gray prong. The decrease of the percentage of gray prongs (Fig. 2) with increasing star size is probably a result of the decrease of the energy available for a gray prong with increasing star size.

Similar considerations can be made by also treating the sparse black prongs as fast knock-on protons,<sup>16</sup> i.e., the dashed curve of Fig. 2.

The difference between the dashed and solid curves in Fig. 2 represents the percentage of stars with sparse black prongs only. The ratio of the percentage of stars with sparse black prongs only to the percentage of stars with a gray prong can be seen from Fig. 2 to increase from  $\sim 0.2$  to  $\sim 3$  from the 1 to 7 prong stars. This also clearly indicates the increasing dissipation of available energy into black prongs with increasing star size and in particular the more or less complete dissipation of the available energy in the large stars. This implies the generation of a nucleonic cascade in a heavy nucleus, since it is to be expected that the light nuclei could split before the dissipation of so much energy.

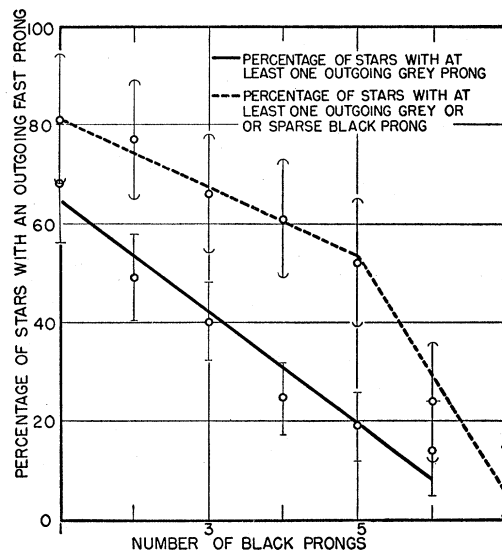


FIG. 2. Percentage of stars with outgoing fast prongs as a function of the number of black prongs, based on 412 stars induced in G-5 emulsion by 350-400 Mev protons.

<sup>16</sup> This will be justified by angular distribution measurements.

TABLE III. Energy of gray proton prongs from proton-induced stars.

Energy in Mev	100-200	200-300	300-400
Number of gray prongs	15	7	4

The clear inference of all these considerations is that in practically all of the stars with less than 7 or 8 black prongs one or more fast nucleons carry away the energy not transferred to the slow nucleons.

The energies of 26 outgoing gray prongs long enough to count at least 500 grains were determined. The results, grouped in 100-Mev intervals, are given in Table III.

A rough estimate of the total energy in the outgoing visible prongs is thus possible. The average disappearance of energy amounted to about one-half the initial energy or about 200 Mev. This means that on the average about half the energy is carried away by neutrons, even in the stars with outgoing gray prongs.

### E. Angular Distribution of Proton Star Prongs

The angular distribution of gray, sparse black, and black prongs was determined in terms of the angle between the beam direction and the prong projection upon a plane parallel to the beam direction. The angular distributions of gray (solid curve) and sparse black (dashed curve) prongs are given in Fig. 3. The black prong angular distribution for all stars and large stars only is given in Fig. 4.

The evaporation prongs are expected to be isotropic and even for excitation energies of 400 Mev to be predominantly confined to the 0-30-Mev energy region.<sup>17</sup> The gray prongs are very sharply projected in the forward direction and are clearly directly ejected knock-ons. The sparse black prongs are less sharply projected, but they also seem to be almost exclusively directly ejected knock-ons. The higher energy gray prongs are more sharply collimated than the lower

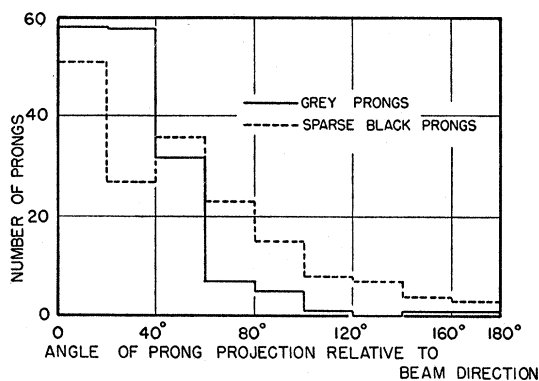


FIG. 3. Angular distribution of gray and sparse black prongs from stars induced by 350-400 Mev proton.

<sup>17</sup> K. J. LeCouteur, Proc. Phys. Soc. (London) A63, 259 (1950).

energy sparse black prongs, in a manner suggestive of a few nucleon-nucleon scatterings.

The black prongs (Fig. 4) could be considered as a superposition of an isotropic and a forwardly projected distribution. The maximum isotropic contribution is obtained by assuming that the average value in the backward 60° region is entirely because of an isotropic component, and extending this value over all angular intervals. In this way one finds that at the most, 60 percent of the black prongs of all stars (curve I) are isotropic.

The evaporation prongs must be isotropically emitted in the center-of-mass system of the thermally evaporating nucleus. If all the momentum of the incoming proton is transferred to the Ag-Br nuclei, the velocity of the nucleus c.m. system would still be small (~5 percent) compared to the velocities corresponding to the characteristic energy (~10 Mev) of the evaporation prongs. However, when we consider that most of the momentum of the incoming proton is carried off by the forwardly collimated directly ejected prongs, the evaporation prongs from Ag-Br nuclei are expected to be isotropically emitted, also in the laboratory system.

Since at most 60 percent of the black prongs of all stars are isotropic, at least 40 percent have an origin other than that of the evaporation products of Ag-Br nuclei.

It has been previously concluded that the stars with 5 or more black prongs should be almost exclusively Ag-Br events. Curve II of Fig. 4 represents the angular distribution of black prongs based on stars with 5 or more black prongs. The maximum isotropic distribution is again found to be about 60 percent. Curve III is based on stars of six or more black prongs in order to assure even further that the light element stars are excluded. Although in this case the statistics are poorer, one still finds the value of 60 percent as the maximum isotropic contribution. Therefore it is clear that at least 40 percent of the black prongs of large Ag-Br stars have a knock-on origin. For the smaller stars, considering the percentage of prongs caused by the light elements, at least 25 percent<sup>18</sup> of the black prongs from Ag-Br stars are knock-ons.

## III. NEUTRON-INDUCED NUCLEAR INTERACTIONS

### A. Exposure

In order to study the high energy proton interactions in more detail it would be desirable to be able to

<sup>18</sup> It was previously shown that at most 20 percent of the stars are due to gelatin nuclei. Because the mean prong number of gelatin stars is about 3 (see reference 15) (probably because of their expected preference for dissociation into  $\alpha$ -particles), no more than 20 percent of the black prongs observed in the emulsion stars originate in light nuclei. Therefore even the extreme assumption that all of these light nuclei black prongs are forwardly projected could only account for half of the observed forwardly projected black prongs. Hence, one concludes that at least 20 percent of the black prongs are knock-ons from Ag-Br nuclei. Since at most 60 percent of the black prongs could be due to

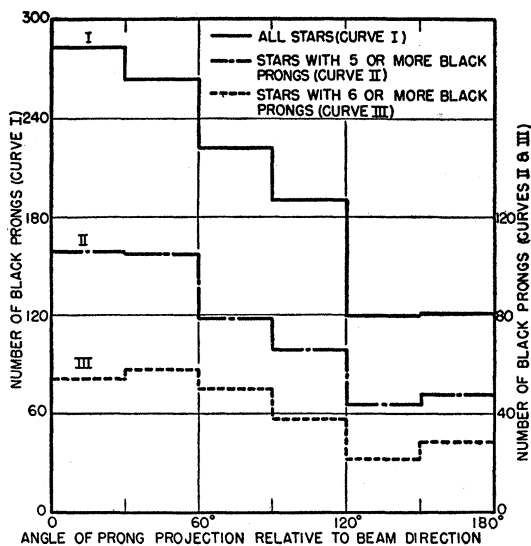


Fig. 4. Angular distribution of black prongs of stars induced by 350-400 Mev protons.

measure directly the characteristics of the emitted neutrons as well as those of the protons. This is obviously impossible with the photographic technique. However, there is a sort of mirror image symmetry predicted by the Goldberger model for the interactions of high energy protons and neutrons of similar energy with the emulsion. This is caused by the fact that there are approximately equal numbers of neutrons and protons (at most 5 neutrons to 4 protons) and it is generally assumed that  $\sigma_{n-n} \approx \sigma_{p-p}$ .<sup>19</sup> Hence it would be expected that the protons directly ejected as a result of neutron bombardment should be equivalent in all respects to the neutrons directly ejected under proton bombardment. And conversely, the protons directly ejected from proton-induced stars should be equivalent to the neutrons directly ejected in neutron-induced stars. Thus the results of the two experiments should be complimentary to each other in a very useful way.

In order to compare the properties of neutron-induced stars with the proton stars, 400 micron G5 plates were exposed to the Nevis high energy neutron beam. The neutron beam was sharply collimated to select only those neutrons directly ejected in the forward direction from a beryllium target bombarded by the proton beam at the maximum energy orbit, which corresponds to a proton energy of 385 Mev.

The energy spectrum of the neutrons was determined from  $\text{CH}_2$  proton recoils with triple coincidence proportional counter telescopes by Goodell.<sup>20</sup>

evaporation of Ag-Br nuclei, it follows that at least 25 percent of the black prongs originating in Ag-Br have a knock-on origin.

<sup>19</sup> This assumption is essentially that of the charge independence of nuclear forces. Its approximate validity can be deduced from the neutron cross-section measurements described in footnotes 9-11.

<sup>20</sup> W. Goodell, Nevis Cyclotron Laboratory, quarterly report, June 15, 1951. The spectrum has a definite peak at about 300 Mev and the average energy is also  $\sim 300$  Mev.

## B. Neutron Star Characteristics

The plates were processed in the same way as the proton plates. The terminology used for the grouping of the proton star prongs will also be used for the neutron star data. In order to avoid confusion with Coulomb scatterings, only those two-prong stars which exhibited a difference in prong grain density were recorded. All three-prong or larger stars were clearly neutron-induced events and were recorded. There is the possibility of the inclusion of background stars induced by cosmic rays. The background because of cosmic-ray stars was estimated to be at most 2 percent of the observed stars, and was neglected.

In Fig. 5 the neutron star, black prong distribution is compared to the proton star distribution curve. The proton curve was normalized to correspond to the same total number of three or more black prong stars. The proton curve is shifted toward higher prong numbers. This is most likely a result of the fact that the average neutron energy (300 Mev) is less than the average proton energy (375 Mev). The magnitude of the shift, about 1-2 prongs, corresponds, as was previously discussed, to about 50-100 Mev. This is in agreement with the difference in the average proton and neutron energies.

In order to compare the numbers and distribution of stars with an outgoing fast (sparse black or gray) prong, the events not recorded in the neutron stars were deleted from the proton star data. Thus all proton stars with either one prong only or with only two black prongs were not considered for the comparison.<sup>21</sup> The remaining events which were observed in both cases are compared in Fig. 6. The proton curve is normalized to

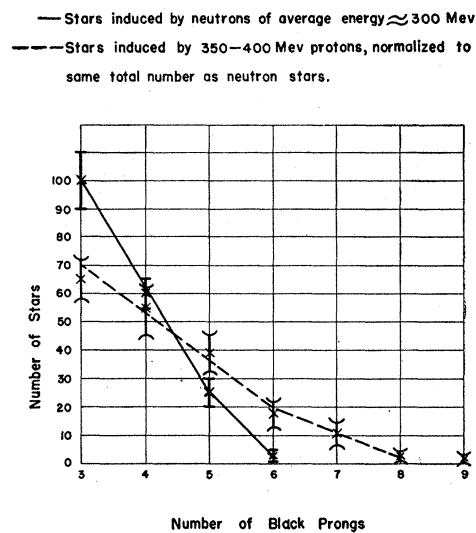


Fig. 5. Comparison of neutron and proton star black prong distributions.

<sup>21</sup> It has to be noted that they represent only about 10 percent of all proton stars.

— Stars induced by neutrons of average energy  $\approx 300$  Mev.  
 - - Stars induced by 350–400 Mev protons.  
 Curve is normalized to same total number of stars (including those without fast prongs) included in the neutron data.

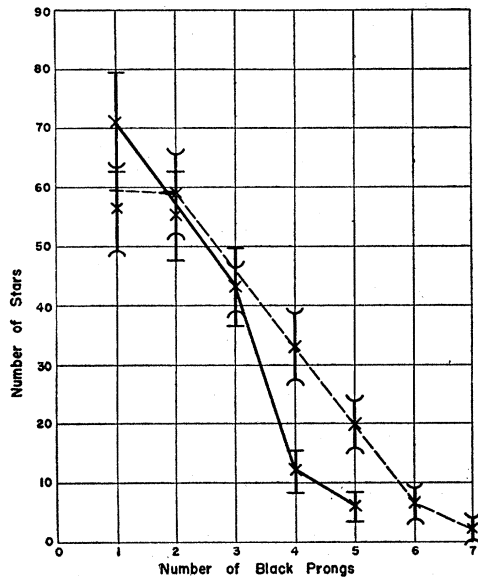


FIG. 6. Comparison of distribution of neutron and proton stars with a fast prong.

correspond to the same number of stars as the neutron curve. The proton curve is again shifted toward higher prong numbers by 1–2 prongs.

Table IV compares characteristic data for proton and neutron stars. The mean numbers of black prongs are the same within statistical limits. Also, the mean numbers of fast ( $>30$  Mev) protons agree within statistics. However, in the case of the neutron stars there are somewhat more sparse black than gray prongs, while the reverse is true for the protons. This could be attributed to the sensitivity of the number of gray ( $>100$  Mev) prongs to the differences in bombarding energy and to the charge of the incoming nucleon.

A comparison of the distribution of events with fast prongs for the proton and neutron stars is made in Table V. Within statistical limits there are practically no differences in the two distributions. The angular distributions of gray, sparse black, and black prongs from neutron and proton-induced stars are compared in Fig. 7(a), (b), and (c). The proton curves were normalized to the same area as that of the neutron curve. The frequency of occurrence of each type of prong for neutron and proton-induced events is given in Table IV. Here again the two distributions are about the same. The energy balance for the neutron events also indicated that about one-half the incoming energy was carried away by neutrons. This result is again similar to the proton star case. Hence we must finally conclude that except for the differences found in the star distribution curves which are attributable to the

lower neutron energy, the many characteristics of the two types of interactions that have been examined are essentially the same.

In view of the previously discussed mirror image symmetry of the two experiments we can conclude that the characteristics of the neutrons emitted in both experiments are identical to those determined for the visible protons.

#### IV. DISCUSSION

The best evidence for the internal nucleonic cascade mechanism will be presented in Part II of this report, where it will be shown that the model calculations are in quantitative agreement with the experimental results. A brief account of these calculations has already been published.<sup>22</sup> However, many of the remarks previously made in various parts of the text provide a direct experimental basis for the interpretation of the so-called stars as mainly the result of an internal nucleonic cascade. It would be difficult to find a simpler explanation of the following facts:

(a) The correlation of the angular distribution of gray ( $>100$  Mev), sparse black (30–100 Mev) and black<sup>23</sup> ( $<30$  Mev) prongs with their respective energy ranges seems to be characteristic of the results of a few single nucleon-nucleon scatterings.

(b) The abundance of black knock-on prongs (at least 25–40 percent) implies a much longer mean free path in nuclear matter for these low energy nucleons than that corresponding to free scattering cross sections, and hence indicates the action of the Pauli exclusion principle which lengthens the mean free path of these low energy nucleons. The large percentage of these low energy knock-ons demonstrates that the usual interpretation of black prongs as mostly a result of the evaporation process is probably wrong.

(c) The steady transfer of energy from the fast nucleons to the black nucleons as star size increases and in particular the almost complete degradation of the energy into black prongs in the largest stars also indicates that the broadness of the distribution curves is determined by cascade fluctuations rather than by

TABLE IV. Comparison of neutron and proton star mean prong numbers.

Type of prong	Black	Sparse black	Gray	Fast (gray and sparse black)
Mean prong No. for proton stars	$3.2 \pm 0.2$	$0.39 \pm 0.04$	$0.46 \pm 0.04$	$0.85 \pm 0.07$
Mean prong No. for neutron stars	$2.9 \pm 0.2$	$0.41 \pm 0.04$	$0.33 \pm 0.05$	$0.74 \pm 0.07$

<sup>22</sup> Bernardini, Booth, and Lindenbaum, Phys. Rev. **83**, 669 (1951).

<sup>23</sup> Only the probable knock-on component is considered.

the fluctuations in the emission of visible prongs in an evaporation process.

(d) The agreement between the observed nuclear transparency for 350–400-Mev protons with the model prediction implies that at least for the first collision the calculated mean free path is correct.

(e) The similarity found for the fast directly-ejected prongs in the neutron and proton-induced interactions, and the implied similarity of the properties of directly ejected neutrons and protons in both types of events is understandable in the case of a cascade of single nucleon-nucleon collisions. The  $n$ - $p$  cross section has been experimentally observed to be symmetrical around  $90^\circ$  in the center-of-mass system, and it is assumed that  $\sigma_{n-n} \approx \sigma_{p-p}$ . Furthermore, there are approximately equal numbers of neutrons and protons in the emulsion nuclei. Hence it is obvious from these symmetry conditions that the cascades of nucleons induced by protons and neutrons of equal energy would be identical in all respects provided that the ejected neutrons and protons are considered as nucleons only, without any distinction between the two. However, in the present experiments only the protons were detected and so in general one would expect an asymmetry between the protons ejected under proton and neutron bombardment. This asymmetry depends inversely upon both the ratio  $\sigma_{n-p}/\sigma_{p-p}$  and the number of collision stages the cascade has gone through inside the nucleus. Using the experimentally determined cross sections it has been estimated that an average of 2–3 collision stages per event would reduce the asymmetry enough to explain the observed similarity of the neutron and proton interactions. This is about what one gets from the model calculations (to be given in Part II).

It has been tacitly assumed throughout the foregoing discussions that the sparse black and gray prongs are predominantly protons. The direct ejection of groups of nucleons such as deuterons and tritons has been recently extensively studied. The theory of these phenomena, or so-called pick-up processes, has been investigated in detail by Chew and Goldberger<sup>24</sup> and Heidmann.<sup>25</sup> A simple description of the theory can be given in the following terms: When a fast nucleon traverses the nucleus, it has a certain probability of passing close enough to a group of nucleons of proper space and

TABLE V. Frequencies of stars *versus* number of their fast prongs.

Number of fast protons	Percentage of stars induced:	
	By neutrons	By protons
0	$30 \pm 4\%$	$29 \pm 3\%$
1	$63 \pm 5\%$	$60 \pm 4\%$
2	$7 \pm 2\%$	$9 \pm 2\%$
3	0%	$2 \pm 1\%$

<sup>24</sup> G. Chew and M. Goldberger, Phys. Rev. **77**, 470 (1950).

<sup>25</sup> J. Heidmann, Phys. Rev. **80**, 171 (1950).

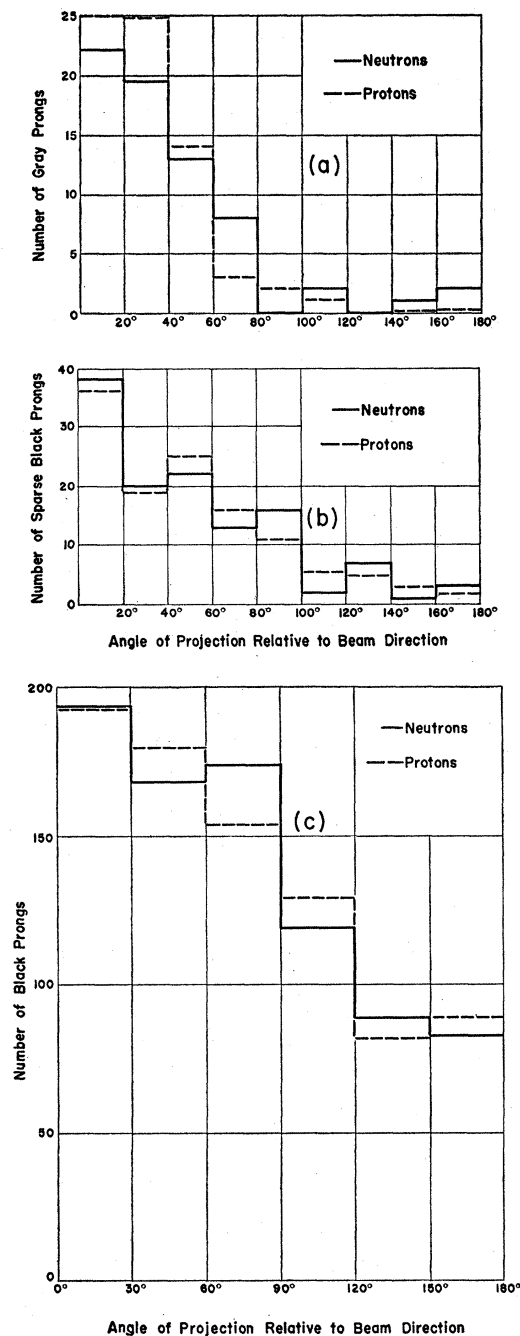


FIG. 7. (a) Comparison of neutron and proton gray prong angular distributions; (b) comparison of neutron and proton sparse black prong angular distributions; (c) comparison of neutron and proton black prong angular distributions.

momentum characteristics to form a stable aggregate such as a deuteron, triton, or alpha-particle. Then there is a corresponding probability for the aggregate to reach the edge of the nucleus undisturbed and escape. For 400-Mev protons this effect is calculated to be negligible.<sup>25</sup> However, the development of nucleonic cascades inside the target nuclei leads to secondary

nucleons in the low energy region ( $\sim 100$  Mev) for which these effects are not negligible.

The mean number of gray plus sparse black prongs is 0.77 (Table II). Taking into account relative numbers of gelatin and Ag-Br stars, we can roughly estimate<sup>26</sup>

<sup>26</sup> J. Hadley and H. York (see reference 4) have investigated deuterons and tritons ejected from carbon, copper, and lead nuclei by 90-Mev neutrons. The ratios of deuteron production cross sections to total inelastic cross sections were found to be 0.12 for carbon, 0.067 for copper, and 0.042 for lead. The cross section for tritons was found to be one-tenth that for deuterons and effectively zero for heavier particles. The assumption that these ratios are the same for the 400-Mev case is a reasonable upper limit. Therefore, one would expect that the mean number of pick-up deuterons and tritons per gelatin stars (using carbon value) would be at the most 0.12 and 0.01, respectively. In Ag-Br we would expect something intermediate between copper and lead or approximately 0.05 and 0.005 as the mean number of deuterons and tritons, respectively.

that at the most 6–8 percent of the gray or sparse black prongs could be pick-up deuterons and 1 percent could be pick-up tritons. These effects are small and do not affect any of the general conclusions reached treating all gray and sparse black prongs as protons.

#### ACKNOWLEDGMENTS

The authors wish to thank Dr. Marietta Blau for several interesting discussions. We also thank Miss Elizabeth Wimmer for her invaluable assistance and cooperation in the photographic plate analysis. Mrs. Josephine Bielk generously aided and advised the authors on plate processing techniques. We also wish to thank the engineering staff of the Nevis Cyclotron Laboratories, in particular Mr. Julius Spiro and Mr. George Rosenbaum, for their help.

## The Formation of a Boundary between Normal-Conducting and Superconducting Metal\*†

M. P. GARFUNKEL‡ AND B. SERIN

*Physics Department, Rutgers University, New Brunswick, New Jersey*

(Received November 6, 1951)

An experiment is described in which a superconducting sample is arranged so that part of it is in the normal state and part of it is superconducting. The boundary surface is thus a single, large area rather than the complicated boundaries that exist between normal and superconducting regions when a sample is in the intermediate state. We find that there is a large difference between the magnetic field at which the superconducting-normal state transition occurs and the magnetic field at which the normal-state-superconducting transition occurs. These results are in agreement with the thermodynamic theory of the phase transition. The thermodynamic theory, coupled with an assumption about the nature of the surface energy between superconducting and normal metal is used to show how the hysteresis determines the ratio of this surface energy to a characteristic dimension of the superconductor. A measure of this ratio is given in the temperature region between 3.37°K and 3.68°K for superconducting tin.

### I. INTRODUCTION

**B**ELOW the critical temperature, the normal state can be restored in a superconductor by the application of a sufficiently large magnetic field.<sup>1</sup> The nature of the transition to the normal state depends on the details of the geometry of the sample relative to the magnetic field. For the special case of a large diameter, infinite cylinder in a uniform, longitudinal magnetic field, the transition occurs abruptly at a definite value of the magnetic field. This value of the field is called the critical field  $H_c$  and for a given metal depends only on the temperature. (At the critical temperature  $T_c$ , the critical field  $H_c$  is zero.) For other geometries, such as an ellipsoid, or a cylinder in a transverse field, the conditions are somewhat different. The magnetic

field is distorted around the edges of the superconductor and thus has greater values at some points on the surface than at others. The complications which arise when the sample does not have a zero demagnetization require the introduction of a new state—the intermediate state.<sup>2</sup> The intermediate state is not a pure state, but is a complicated structure of superconducting and normal domains.<sup>3–5</sup> The domains were observed by Meshkovsky and Shalnikov<sup>5</sup> to have diameters of about 0.1 cm.

Since all experiments to determine the critical field are carried out on finite cylinders, which have nonzero demagnetization, the transition from the superconducting to the normal state in a longitudinal field for such cylinders occurs with the formation of an intermediate state, usually at the ends of the cylinder. Since the intermediate state consists of small domains of superconducting and normal regions, the transition

\* This work has been supported by the joint program of the ONR and AEC, the Rutgers University Research Council, and by the Radio Corporation of America.

† Based on the Ph.D. thesis submitted by M. P. Garfunkel to the Graduate Faculty of Rutgers University.

‡ Now at Westinghouse Research Laboratories, East Pittsburgh, Pennsylvania.

<sup>1</sup> H. Kammerlingh Onnes, *Leiden Comm.* **122b** (1911); *Leiden Comm.* **124c** (1911); *Leiden Comm. Suppl.* **35** (1913).

<sup>2</sup> C. J. Gorter and H. Casimir, *Physica* **1**, 305 (1934).

<sup>3</sup> L. Landau, *Nature* **141**, 688 (1938).

<sup>4</sup> A. Shalnikov, *J. Phys. U.S.S.R.* **9**, 202 (1945).

<sup>5</sup> A. Meshkovsky and A. Shalnikov, *J. Phys. U.S.S.R.* **11**, 1 (1947).